Journal of Sciences, Islamic Republic of Iran 29(1): 53 - 65 (2018) http://jsciences.ut.ac.ir
University of Tehran, ISSN 1016-1104

Origin of Lherzolitic Peridotites in Ab-Bid Ultramafic Complex (Hormozgan Province); Products of Mantle Metasomatism or Partial Melting Processes?

M. Mohammadi*, H. Ahmadipour, and A. Moradian

Department of Geology, Faculty of of Sciences , University of Shahid Bahonar, Kerman, Islamic Republic of Iran

Received: 18 October 2016 / Revised: 3 January 2017 / Accepted: 13 February 2017

Abstract

Lherzolite is one of the main units in the Ab-Bid ultramafic complex from Esfandagheh-HadjiAbad coloured mélange (South of Iran). The complex contains harzburgite, dunite, lherzolite and pyroxenite dykes and the lherzolites mainly occur in the margins. In the field, lherzolites occur as weakly foliated coarse-grained peridotites with shiny pyroxene grains and cut by neumerous pyroxenitic veins. Textural features such as elongation and undoluse extinction of minerals and porphyroclastic grains indicate that the lherzolites were part of the upper mantle and experienced high P-T deformational events. Mineral chemistry data such as Cr# values in spinels (10/33-14/04) and fo contents of olivines (90/49-93/51) from the Ab-Bid lherzolites suggest that these rocks belong to the mantle. Evidences such as CaO (1/18-3/23) and MgO (39/53-43/65) contents of whole rock compositions, Cr# (10/33-14/04) and Mg# (74/20-78) values of spinels, besides textural features and REE normalized patterns show that they have past a complex petrological history. At the first stage, they have partially melted (< 10%) in an abyssal environment, then, they refertilized by ascending melts and enriched in LREE. Tectonomagmatic discrimination diagrams indicate that Ab-Bid lherzolites belong to the abyssal peridotites and their petrogenetic evolutions are similar to those from MOR type peridotites. Our data document the dependence of Esfandagheh-HadjiAbad coloured mélange to the Neotethyan oceanic lithosphere in the south of Iran.

Keywords: Ab-Bid ultramafic complex; Esfandagheh-HadjiAbad coloured mélange; Hormozgan province; Lherzolite; Mantle metasomatism.

Introduction

Lherzolites are the essential parts of many ophiolitic associations and ultramafic complexes all around the world [12]. There are different ideas about genesis and petrological evolution of these mantle peridotites [3]. Some authors [9] believe that the lherzolites are the more fertile parts of the upper mantle which have not been affected by partial

* Corresponding author: Tel:+983431322237; Fax: +983431322222; Email:mahta_6024@yahoo.com, mahdyeh.mohammadiye@pnu.ac.ir

melting. As stated by Bodinier [5] chemical and mineralogical variations in mantle rocks are attributed to variable degrees of partial melting. In fact, the most fertile lherzolites (with 15% clinopyroxene) are interpreted as primitive mantle only weakly affected by partial melting, while, the harzburgites (with less than 5% clinopyroxene) show high degrees of partial melting and melt extraction. So, these fertile lherzolites together with chondritic meteorites, were used to infer the composition of the Earth's primitive mantle [19]. In many ultramafic suits such as Lanzo, Italy [5]; Lherz, France [5] and Western Gneiss Region, Norway [8], the lherzolites often considered as residual mantle containing remnants of pristine material. However, many cases show that the lherzolites may also derived from combined processes of partial melting and igneous refertilization. Plagioclase lherzolites, in particular, are interpreted as products of impregnation of previously depleted peridotites by percolating melts [28]. Müntener [22] stated that the plagioclase peridotites in western Alps and Apennines have been formed by a reaction between extending lithosphere from embryonic ocean basins and upwelling asthenospheric melts. Spinel lherzolites from the Ronda Massif (S Spain) attributed to refertilization of subcontinental lithosphere [18].

The Ab-Bid peridotitic complex (Hormozgan province, Iran), is a large ultramafic massif (10 km x 4/5 km) dominantly composed of harzburgites, but in marginal parts, it contains some distinctive lherzolite outcrops with different field and perographical characteristics. The aims of this work, are 1) presentation of field, petrography, mineral and whole rock chemistry of these lherzolites for the first time and 2) using these data in order to clarifying petrological evolutions of these rocks and the other rock associations from the Ab-Bid complex.

Materials and Methods

Major – element in whole rocks were analyzed at the laboratory of Acts lab in Canada with code 4B2 – std options A 1 g. Samples are digested with aqua regia and diluted to 250 ml volumetrically. Appropriate international reference materials for the metals of interest are digested at the same time. The samples and standards are analyzed on Thermo ICAP 6500 ICP. Minor and trace element (Ti, Sr, Zr, … and Rare earth elements) concentrations in whole rock were analyzed by solution ICP MS (mass spectrometry) at the same laboratory with method 4 litho – research. Quantitative chemical analysis (Electron microprobe analysis) was performed at University of British Columbia, Canada, in the Department of Earth, Ocean and Atmospheric Sciences by using a fully-automated Cameca SX50 Scanning Electron Microprobe with 4 vertical wavelength-dispersion X-ray spectrometers and a fully-integrated SAMx energy-dispersion X-ray spectrometer. One of the spectrometers has two layered dispersion elements (W/Si, Ni/C), which allow the quantitative analysis of the light elements (F, O, N, C, B). There are standards for virtually all of the elements and common alloys. The instrument can produce X-ray element maps from EDS or WDS spectrometers, back scattered electron images, and secondary electron images. All electron microprobe analyses were measured with the following operating conditions: voltage, 15 kV; beam current, 20 nA; peak count-time, 20 s; background count-time, 10 s; spot diameter, 5 μm.

Results

Geological setting

Ab-Bid ultramafic complex is one of the mantle peridotite bodies occuring in the Esfandagheh-Hadjiabad coloured mélange at the south of Iran [2]. The complex is an elliptical relatively unaltered peridotite body which has been emplaced in the Esfandagheh-Hadjiabad ophiolite mélange. This ophiolitic mélange locates at the northern border of the Zagros thrust in this area and forms south-eastern parts of Kermashah-Neyriz ophiolite belt [31]. Esfandaghe-Hadji Abad ophiolite mélange (which hosts Ab-Bid ultramafic complex and the studied lherzolites), is a part of Tethyan ophiolitic belt. Many authors believe that ophiolitic complexes in this belt have been formed in suprasubduction zone setting [38; 25; 11]. Researchers such as Alavi [1] and Mohajell [21] believe that this belt shows the remnants of Neotethys oceanic crust which have been detached during the late Cretaceous. The last mapping of the Esfandagheh-Hadjiabad coloured mélange [2] has revealed that the Ab-Bid ultramafic complex emplaced into the serpentinites, Cretaceous meta-limestones and radiolarian cherts. All contacts are tectonized and the rock units show a typical ophiolitic lithological assemblages. The studied lherzolites comprise marginal parts of the Ab-Bid ultramafic complex.

Field relationships

The Ab-Bid massif crops out as an elongate, NW-SE-trending lens 10 km long and 4/5 km wide between the Sanandaj-Sirjan metamorphic zone at the

north-east and the Zagros thrust zone in the south-west [Fig. 1] [2]. The contacts of the massif are faulted with several meters wide schistose serpentinized peridotites, suggests that the Ab-Bid complex has been emplaced into the other rock units as a solid mass. The massif mainly contains of harzburgites which have been acted as the host of the other lithological units. These rocks appear as homogeneous coarse-grained outcrops without distinct layering or foliation. They have various amounts of shiny orthopyroxene crystals (up to 1 cm in diameter) and dispersed small grains spinels. They show sharp and tectonized contacts with all the rock units and the highest degrees of serpentinization have been occured in these contacts. There are two shapes of dunites in the Ab-Bid. The first one form large massive dunites in the north-west and east of Ab-Bid complex and contain several chromitite ore deposits [Fig. 1]. The

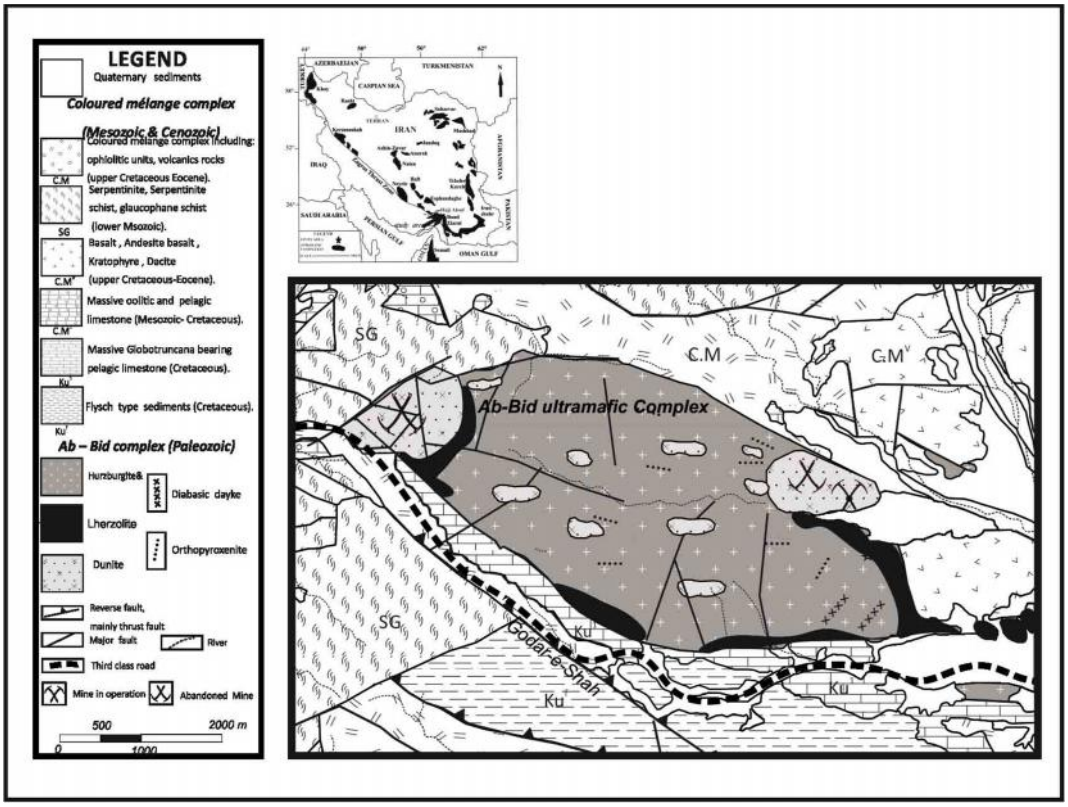

Figure 1. a) Distribution of Iranian ophiolites and location of the studied area in Iran. b) Geological map of Ab-Bid ultramafic complex [2].

Figure 2. a) Occurrence of Ab-Bid lherzolites and harzburgites in the Esfandaghe-Hadji Abad coloured mélange. b) Ab-Bid lherzolite outcrop with the pyroxenite vein.

second dunites are decimeter-meter wide dunitic dykes crosscutting harzburgites throughout the massif. They have intruded in various trends and contain sporadic millimeter-sized spinels.

The lherzolites (investigated in this work) occur in the south and south-west of the massif [Fig. 2a]. The contacts with the harzburgites are often sharp, tectonized and serpentinized.The lherzolites are generally coarse-grained rocks without any foliation and constitute about 15 percent of the Ab-Bid massif. In the field, they have not distinctive layering, but shiny pyroxene grains (ortho- and clino) with up to 6 milimetrs in diameters are found in them. There are a lot of centimeter-sized pyroxenite dykes in this unit

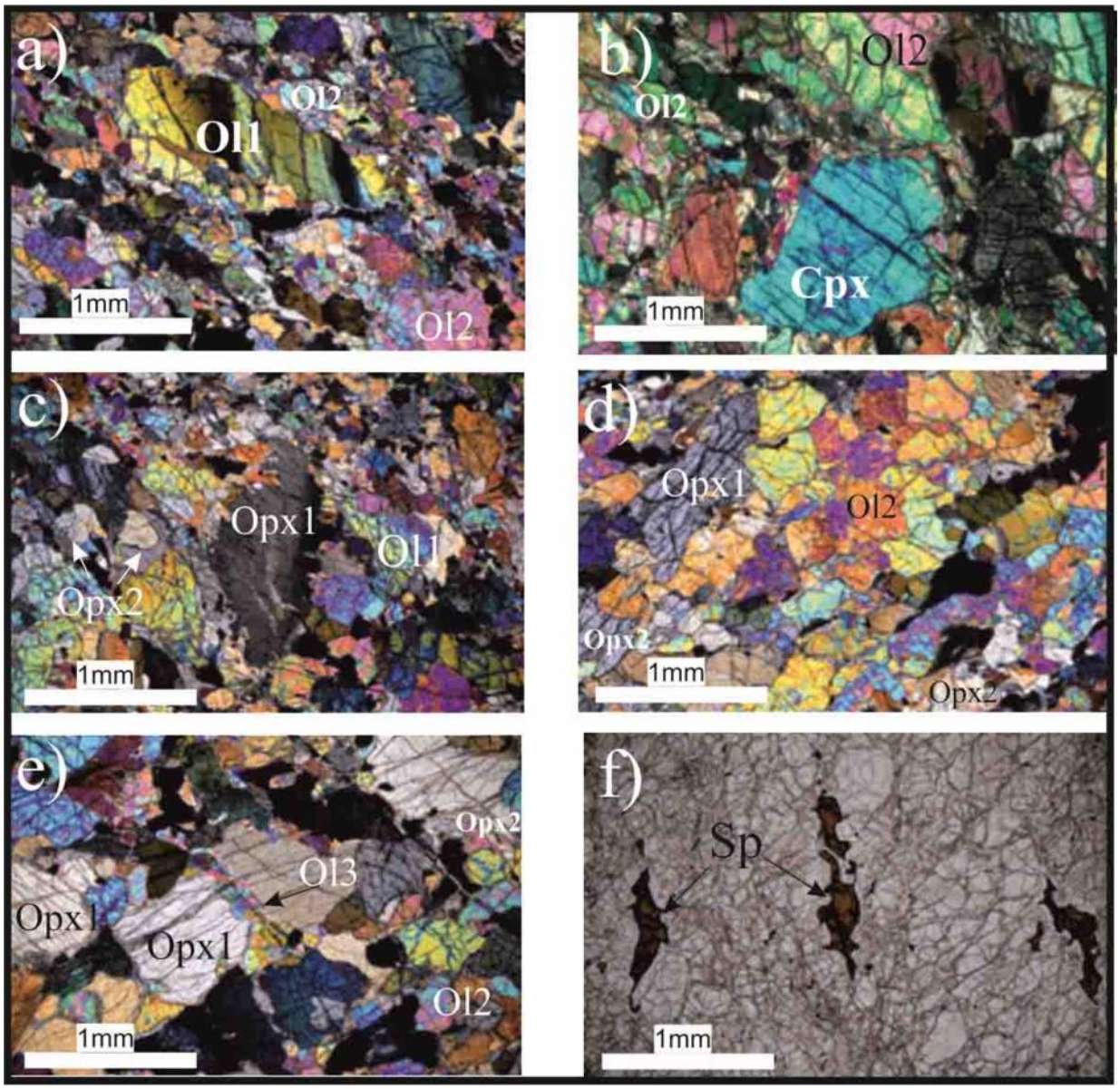

Figure 3. Photomicrographs of Ab-Bid lherzolites. a) Deformed olivine porphyroclast with undoluse extinction (Ol1) enclosed by second generations of fine-grained olivines, clino- and orthopyroxenes in a porphyroclastic texture. Interstitial orthopyroxene crystals (Opx2) are seen in the lower part of the photo. b) Granular texture in Ab-Bid lherzolites with large deformed clinopyroxene crystals. c) Orthopyroxene porphyroclast (Opx1) with curved boundaries. Second generation of olivines (Ol2) and orthopyroxenes (Opx2) observe in its margins. d) Granular textured olivine neoblasts with triple junction boundaries. e) Third generation of olivine grains (Ol3) which have been formed in orthopyroxene porphyroclast (Opx1) probably due to incongruent melting of orthopyroxene during melt-rock interaction. f) Interstitial greenish-brown spinel grains in the Ab-Bid lherzolites.

[Fig. 2b]. The dykes have been intruded in different directions and it seems that they followed the fracture systems. Around the dykes, lherzolites have serpentinized, but in other parts, the host rocks are unaltered. In the field, Ab-Bid lherzolites can be easily distinguished by their yellow-pale brown color against dark red-brown color of the harzburgites.

Petrography

Ab-Bid massif perididtites are fresh with usually less than 10% secondary serpentine [Fig. 3], which occurs as veinlets or is locally pervasive. The harzburgites contain 65-75% Ol, 12-25% Opx, 1-3% Cpx, less than 2% Sp. At the thin-section scale, they display a porphyroclastic microstructure, characteristic of deformation by dislocation creep. A weak foliation and lineation are marked by elongated spinels and olivine porphyroclasts with curvilinear grain boundaries, undulose extinction, and subgrain boundaries. Orthopyroxenes, as well as small clinopyroxenes, show irregular shapes and undulose extinction. In these rocks, large porphyrocastic olivine grains commonly display undulatory extinction and kink banding with curved boundaries, and intracrystalline deformation features are still observed in them, but the neoblastic olivines are found as small undeformed crystals with straight grain boundaries.

Modal compositions in Ab-Bid lherzolites are: 50-65% Ol, 20-25% Opx, 10-16% Cpx, 2-4% Sp. The lherzolites are characterized by coarse-grained granular texture, but in some samples, they show porphyroclastic texture with porphyroclasts of olivine and orthopyroxene up to1 cm across in an equigranular matrix of smaller olivines and pyroxenes [Fig. 3a]. In these rocks, olivine occurs as large porphyroclastic deformed grains (Ol1) (up to 7 mm in size) with deformation twining and elongation in which high temperature deformation recorded [Fig. 3a]. In addition, in the studied lherzolites, there are some small neoblastic olivine grains (Ol2) without any deformation features which have been formed around orthopyroxene and olivine porphyroclasts [Fig. 3d]. Neoblastic olivines are polygonal with straight grain boundaries and triple junctions [Fig. 3d]. Third generation of olivines (Ol3) occur as small grain aggregates which have been formed within or between orthopyroxene porphyroclasts [Fig. 3e]. Clinopyroxene crystals are either independent deformed porphyroclasts (up to 4 mm in size) [Fig. 3b] or occur as small undeformed grains (~0.4 mm). The first group show undulatory extinction and some of them contain fine orthopyroxene exsolution lamellae. Orthopyroxene occurs either as deformed coarse-grained porphyroclasts (up to 10 mm in size) (Opx1) [Fig. 3c,d,e] or neoblastic undeformed fine-grained crystals (up to 0.5 mm in size) (Opx2) which have been formed between the first generation ones probably by recrystallization processes [Fig. 3,c,d]. Opx1 gains may also contain exsolutions of clinopyroxene and are typically in spatial association with spinel [Fig. 3e]. Some clinopyroxenes and orthopyroxenes are slightly folded or kinked and can also include small grains of olivine. Orthopyroxene porphyroclasts partly replaced by fine-grained secondary olivines [Fig. 3c],

Spinel, the content of which ranges from 0.5 to 2 vol%, is usually brownish-green [Fig. 3f], although some spinels tend to be dark-red and more opaque. These minerals are interstitial and display a weak shape-preferred orientation [Fig. 3f]. They have placed between olivines and pyroxenes and their grain size varies from 0.5 mm to 2 mm. Some of orthopyroxene crystals embayed by secondary olivine [Fig. 3c] and interstitial extensions of spinel between adjacent crystals are frequent [Fig. 3f].

Mineral chemistry

Overally, mineral compositions in the Ab-Bid lherzolites are magnesian and different mineral generations have similar compositions. The compositions of olivines are very similar and show a little variations.They have fo values ranging from 90/49 to 93/51 with NiO contents from 0/28 to 0/45 wt.% [Table 1]. In MnO vs fo diagram (not shown), the most Ab-Bid lherzolitic olivines fall in the field of olivine mantle array. Mg# vs NiO contents of olivines from Ab-Bid lherzolites [Fig. 4a] show that the host rocks are refractory mantle peridotites.

Spinels from the Ab-Bid lherzolites have a typical Mg# [=100×Mg/(Mg+Fe)] between 73/20 and 78 with Cr# [= 100 × Cr/(Cr + Al)] varying from 10/33 to 14/04, TiO_2 content for these spinels varies from 0/02 to 0/11 wt% [Table 2]. Compositionally, they are chromespinel and in Al_2O_3 vs Cr_2O_3 diagram [Fig. 4c], these minerals place in the mantle array field. Besides, as shown in figure 4b, the studied spinels belong to the fertile mantle peridotites.

Orthopyroxenes in the studied lherzolites have uniform compositions (Mg# between 91/05 and 93/01) with Al_2O_3 and Cr_2O_3 contents varying from 1/92 to 4/79 and 0/13 to 0/45, respectively (Table 4). They are enstatite and both porphyroclasts and smaller ones have similar compositions. In Mg# vs Al_2O_3 diagram for the orthopyroxenes [Fig. 5a], Ab-Bid orthopyroxenes fall between fertile and refractory mantle peridotites.

Table 1. Representative olivine compositions from Ab–Bid lherzolites (Lhr: Lherzolite).

Sample	**R15**	**R15**	**R15**	**R15**	**R15**	**R15**	**Z18**	**Z18**	**Z18**	**Z18**	**Z18**	**Z18**
Phase	Ol	Ol	Ol	Ol	Ol	Ol	Ol	Ol	Ol	Ol	Ol	Ol
Rock type	Lhr	Lhr	Lhr	Lhr	Lhr	Lhr	Lhr	Lhr	Lhr	Lhr	Lhr	Lhr
SiO_2	41.91	41.37	42.21	42.09	41.19	41.68	40.37	40.41	39.89	40.13	40.08	40.57
Al_2O_3	0.01	0.00	0.00	0.00	0.01	0.00	0.00	0.01	0.01	0.00	0.01	0.01
TiO_2	0.00	0.00	0.00	0.03	0.02	0.03	0.02	0.00	0.00	0.01	0.02	0.00
Cr_2O_3	0.00	0.02	0.00	0.00	0.02	0.00	0.02	0.00	0.00	0.00	0.04	0.00
FeO	8.30	9.22	8.25	9.23	9.06	9.35	9.00	9.53	9.25	9.62	8.87	9.27
MnO	0.16	0.06	0.09	0.05	0.20	0.13	0.17	0.13	0.14	0.13	0.13	0.13
MgO	50.21	49.95	50.70	50.74	49.82	50.82	49.70	49.82	49.98	50.26	50.15	49.65
CaO	0.03	0.00	0.01	0.00	0.03	0.00	0.00	0.02	0.00	0.02	0.00	0.14
NaO	0.00	0.00	0.00	0.00	0.00	0.03	0.03	0.05	0.01	0.00	0.03	0.00
NiO	0.35	0.37	0.44	0.35	0.40	0.35	0.42	0.39	0.40	0.45	0.45	0.42
Total	100.95	101.00	101.71	102.49	100.75	102.39	99.36	100.06	99.50	100.43	99.49	99.86
Si	1.01	1.00	1.01	1.01	1.00	1.00	0.99	0.99	0.98	0.98	0.98	0.99
Ti	0.00	0.00	0.00	0.00	0.00	0.00	0.00	0.00	0.00	0.00	0.00	0.00
Al	0.00	0.00	0.00	0.00	0.00	0.00	0.00	0.00	0.00	0.00	0.00	0.00
Cr	0.00	0.00	0.00	0.00	0.00	0.00	0.00	0.00	0.00	0.00	0.00	0.00
Fe^3	0.00	0.00	0.00	0.00	0.00	0.00	0.02	0.03	0.04	0.05	0.03	0.01
Fe^2	0.17	0.19	0.17	0.18	0.18	0.18	0.17	0.17	0.15	0.15	0.15	0.18
Mn	0.00	0.00	0.00	0.00	0.00	0.00	0.00	0.00	0.00	0.00	0.00	0.00
Mg	1.81	1.81	1.82	1.81	1.81	1.81	1.82	1.81	1.83	1.82	1.83	1.81
Ca	0.00	0.00	0.00	0.00	0.00	0.00	0.00	0.00	0.00	0.00	0.00	0.00
Mg#	91.52	90.62	91.63	90.74	90.74	90.86	91.53	91.46	92.52	92.40	92.53	91.18
Fo	91.52	90.62	91.63	90.74	90.74	90.86	91.53	91.46	92.52	92.40	92.53	91.18
Fa	8.48	9.38	8.37	9.26	9.26	9.14	8.47	8.54	7.48	7.60	7.47	8.82

Standars are as Table 3.

Table 2. Representative spinel compositions from Ab–Bid lherzolites.

Sample	**R15**	**R15**	**R15**	**R15**	**R15**	**R15**	**R15**	**Z18**	**Z18**	**Z18**	**Z18**	**Z18**
Phase	Sp	Sp	Sp	Sp	Sp	Sp	Sp	Sp	Sp	Sp	Sp	Sp
Rock type	Lhr	Lhr	Lhr	Lhr	Lhr	Lhr	Lhr	Lhr	Lhr	Lhr	Lhr	Lhr
SiO_2	0.00	0.00	0.00	0.00	0.00	0.00	0.00	0.00	0.01	0.00	0.03	0.02
Al_2O_3	56.72	58.60	54.80	55.12	55.61	55.10	55.28	57.28	56.26	56.13	56.27	55.25
TiO_2	0.05	0.02	0.06	0.04	0.05	0.06	0.10	0.11	0.05	0.04	0.04	0.02
Cr_2O_3	11.59	10.47	12.82	12.56	12.57	12.96	13.46	10.17	10.95	11.09	11.75	11.53
FeO	11.56	11.64	12.57	11.71	12.65	13.26	13.06	12.84	12.97	12.82	13.43	12.66
MnO	0.11	0.05	0.11	0.13	0.12	0.10	0.14	0.09	0.05	0.05	0.12	0.12
MgO	20.19	20.33	19.22	19.16	19.53	19.29	19.30	19.42	19.30	19.25	19.15	18.96
CaO	0.00	0.04	0.04	0.00	0.01	0.00	0.00	0.00	0.01	0.01	0.00	0.00
NiO	0.31	0.29	0.44	0.32	0.32	0.37	0.30	0.36	0.39	0.34	0.35	0.37
Na_2O	0.00	0.00	0.07	0.00	0.01	0.03	0.01	0.00	0.00	0.00	0.00	0.00
K_2O	0.02	0.01	0.02	0.00	0.01	0.00	0.02	0.00	0.00	0.00	0.00	0.00
Total	100.54	101.44	100.17	99.04	100.87	101.17	101.68	100.08	99.78	99.54	100.95	98.71
Si	0.00	0.00	0.00	0.00	0.00	0.00	0.00	0.00	0.00	0.00	0.00	0.00
Ti	0.00	0.00	0.00	0.00	0.00	0.00	0.00	0.00	0.00	0.00	0.00	0.00
Al	1.73	1.76	1.70	1.72	1.71	1.69	1.69	1.75	1.73	1.73	1.72	1.73
Cr	0.24	0.21	0.27	0.26	0.26	0.27	0.28	0.21	0.23	0.23	0.24	0.24
Fe^3	0.03	0.02	0.03	0.02	0.03	0.04	0.03	0.03	0.04	0.03	0.03	0.03
Fe^2	0.22	0.23	0.25	0.24	0.24	0.25	0.25	0.25	0.25	0.25	0.26	0.25
Mn	0.00	0.00	0.00	0.00	0.00	0.00	0.00	0.00	0.00	0.00	0.00	0.00
Mg	0.78	0.77	0.75	0.76	0.76	0.75	0.75	0.75	0.75	0.75	0.74	0.75
Cr#	12.06	10.70	13.57	13.26	13.17	13.63	14.04	10.65	11.55	11.70	12.29	12.28
Mg#	78.00	77.46	75.46	75.74	75.88	75.01	74.70	75.26	75.26	75.27	74.20	75.03

Standars are as Table 3.

Clinopyroxenes from the Ab-Bid lherzolites show high Mg#values (91/75 – 93/92) along with Al_2O_3, Cr_2O_3, TiO_2 contents varying from 2/04 to 4/82 wt%, 0/16 to 0/96 wt% and 0/1 to 0/98 wt%, respectively [Table 3]. They are diopside and two shapes of the clinopyroxenes show similar chemical compsitions. In

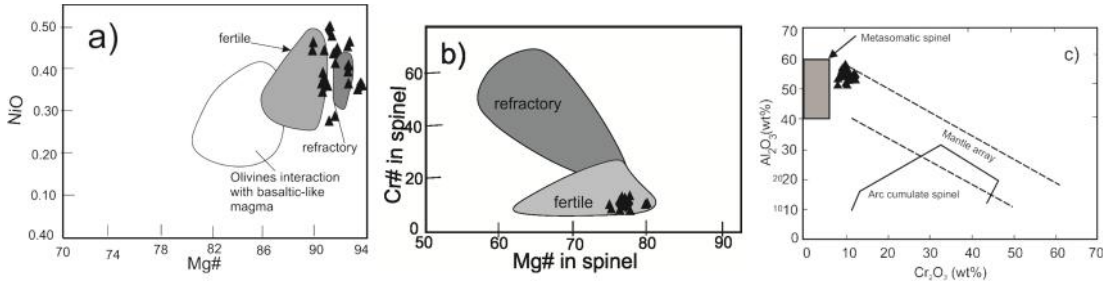

Figure 4. Chemical variations of spinels and olivines from Ab-Bid lherzolites. a) Mg# vs NiO in olivines from Ab-Bid lherzolites. Data sources: Fertile and refractory mantle from [40], Olivine interactions with basalt-like magma from [39]. b) In Mg# vs Cr# diagram, spinel from Ab-Bid lherzolites fall in the fertile mantle field. Data sources are as Fig. 4a. c) The studied spinels fall in the mantle array field and their compositions are close to the metasomatic spinels. Fields from [17].

the Al_2O_3 vs Mg# [=100×(Mg/(Mg+Fe))] diagram [Fig. 5b], these minerals fall in the high pressure field clinopyroxenes.

Whole rock chemistry

Lherzolites from Ab-Bid ultramafic complex show variable degrees of serpentinization (LOI: 0/61 – 4/56%) [Table 5], but most of them are fresh and their Mg# varies between 89/94 and 90/47. Ab-Bid lherzolites have relatively high Al_2O_3 and CaO values (3/29 And 90/47% respectively). So, they are comparable with the mantle lherzolites worldwide [29]. These rocks are enriched in iron (Fe_2O_3(T) content averaging 8/86 with values as high as 9/21 %), however in Cr vs Al_2O_3 diagram [Fig. 6] they fall in the field of reference mantle peridotites.

Table 3. Representative clinopyroxene compositions from Ab–Bid lherzolites.

Sample	**Z18**	**Z18**	**Z18**	**Z18**	**Z18**	**Z18**	**Z18**	**Z18**	**Z18**	**Z18**	**Z18**	**Z18**
Phase	CPX	CPX	CPX	CPX	CPX	CPX	CPX	CPX	CPX	CPX	CPX	CPX
Rock type	Lhr	Lhr	Lhr	Lhr	Lhr	Lhr	Lhr	Lhr	Lhr	Lhr	Lhr	Lhr
SiO_2	54.03	52.92	52.17	52.44	52.65	53.01	52.84	52.84	51.34	52.58	51.49	51.08
TiO_2	0.17	0.24	0.30	0.25	0.43	0.27	0.30	0.27	0.35	0.29	0.40	0.44
Al_2O_3	2.04	3.10	4.27	3.68	3.86	3.02	3.38	3.50	4.82	3.86	4.54	4.75
Cr_2O_3	0.16	0.51	0.56	0.45	0.67	0.45	0.51	0.63	0.82	0.85	0.82	0.76
FeO	2.01	2.10	2.17	2.24	2.09	1.95	2.15	2.11	2.07	2.08	2.04	2.00
MnO	0.08	0.06	0.08	0.07	0.03	0.11	0.04	0.10	0.03	0.09	0.08	0.04
MgO	17.39	16.52	16.41	16.56	16.17	16.93	16.50	16.43	16.24	16.28	16.03	16.12
CaO	23.79	23.45	23.50	23.36	23.62	23.64	23.64	23.70	23.23	23.59	23.61	23.25
Na_2O	0.41	0.57	0.64	0.60	0.51	0.50	0.58	0.52	0.72	0.66	0.61	0.64
K_2O	0.01	0.00	0.01	0.00	0.00	0.00	0.00	0.01	0.01	0.00	0.00	0.00
NiO	0.02	0.00	0.02	0.09	0.00	0.02	0.05	0.04	0.00	0.07	0.06	0.04
Total	100.15	99.55	100.32	99.84	100.06	100.00	100.05	100.18	99.90	100.44	99.82	99.31
Si	1.95	1.93	1.89	1.90	1.91	1.92	1.92	1.91	1.86	1.90	1.87	1.87
Ti	0.00	0.01	0.01	0.01	0.01	0.01	0.01	0.01	0.01	0.01	0.01	0.01
Al	0.09	0.13	0.18	0.16	0.17	0.13	0.14	0.15	0.21	0.16	0.19	0.20
Cr	0.00	0.01	0.02	0.01	0.02	0.01	0.01	0.02	0.02	0.02	0.02	0.02
Fe^3	0.02	0.02	0.06	0.05	0.01	0.04	0.03	0.03	0.07	0.04	0.06	0.06
Fe^2	0.04	0.04	0.01	0.02	0.06	0.02	0.03	0.04	-0.01	0.02	0.01	0.00
Mn	0.00	0.00	0.00	0.00	0.00	0.00	0.00	0.00	0.00	0.00	0.00	0.00
Mg	0.94	0.90	0.88	0.90	0.87	0.91	0.89	0.89	0.88	0.88	0.87	0.88
Ca	0.92	0.92	0.91	0.91	0.92	0.92	0.92	0.92	0.90	0.91	0.92	0.91
Na	0.03	0.04	0.05	0.04	0.04	0.04	0.04	0.04	0.05	0.05	0.04	0.05
Mg#	93.92	93.75	92.63	92.78	92.55	93.81	93.68	92.71	93.62	93.62	92.55	93.62
Cr#	4.89	7.14	10.00	5.88	10.53	7.14	6.67	11.76	8.70	11.11	9.52	9.09
Wo	48.54	49.41	50.53	49.84	49.64	49.48	49.88	49.82	51.02	50.40	51.24	50.96
En	49.38	48.43	49.08	49.16	47.29	49.32	48.43	48.07	49.63	48.40	48.41	49.14
Fs	2.07	2.16	0.39	0.99	3.07	1.20	1.70	2.10	0.65	1.21	0.35	0.10

Standards: SiO_2 (diopside), TiO_2 (rutile,Astimex, synthetic), Al_2O_3 (disthen, MAC),Cr_2O_3 (chromium Oxide, Astimex, synthetic), FeO (fayalite. USNM,Rockport), MnO (rhodonite, Astimex. Franklin, USA), MgO (Olivine,USNM, San Carlos), CaO (diopside), NiO (NiO, synthetic), Na_2O (jadeite), K_2O (K-Felspar). Opxt=Orthopyroxenite. Fe^{3+} and Fe^{2+} are calculate from stoichiometry. Mg# =100Mg/ (Mg+Fe^{2+}). Wo =Ca/ (Ca+Mg+Fe^{2+}). En= Mg/ (Ca+Mg+Fe^{2+}). Fs=Fe^{2+}/ (Ca+Mg+Fe^{2+}).

Table 4. Representative orthopyroxene compositions from Ab–Bid lherzolites.

Sample	**Z18**	**Z18**	**Z18**	**Z18**	**Z18**	**Z18**	**Z18**	**Z18**	**Z18**	**Z18**	**Z18**	**Z18**
Phase	OPX	OPX	OPX	OPX	OPX	OPX	OPX	OPX	OPX	OPX	OPX	OPX
Rock type	Lhr	Lhr	Lhr	Lhr	Lhr	Lhr	Lhr	Lhr	Lhr	Lhr	Lhr	Lhr
SiO_2	55.98	56.07	56.29	56.39	55.07	56.39	54.60	55.11	55.83	54.46	55.76	55.38
TiO_2	0.07	0.04	0.05	0.07	0.08	0.06	0.06	0.03	0.05	0.09	0.08	0.04
Al_2O_3	3.04	1.93	2.37	2.31	3.62	2.41	4.18	3.88	3.63	4.79	3.24	3.64
Cr_2O_3	0.26	0.14	0.17	0.18	0.28	0.18	0.45	0.40	0.32	0.37	0.30	0.37
FeO	6.75	7.04	6.76	6.96	6.64	6.95	6.75	6.78	6.47	6.64	6.79	6.55
MnO	0.16	0.12	0.15	0.17	0.16	0.14	0.17	0.14	0.13	0.19	0.15	0.13
MgO	34.14	34.63	34.66	34.43	33.67	34.33	33.78	33.56	33.77	33.32	34.14	33.94
CaO	0.28	0.20	0.21	0.30	0.36	0.26	0.23	0.40	0.33	0.44	0.29	0.52
Na_2O	0.00	0.01	0.05	0.01	0.04	0.02	0.01	0.04	0.00	0.03	0.02	0.01
K_2O	0.00	0.00	0.01	0.01	0.01	0.00	0.00	0.00	0.00	0.00	0.00	0.00
NiO	0.12	0.04	0.07	0.13	0.07	0.06	0.07	0.08	0.09	0.04	0.05	0.05
Total	100.79	100.42	100.91	100.97	100.10	100.88	100.48	100.52	100.56	100.53	100.93	100.76
Si	1.92	1.93	1.92	1.93	1.90	1.93	1.88	1.89	1.92	1.87	1.91	1.90
Ti	0.00	0.00	0.00	0.00	0.00	0.00	0.00	0.00	0.00	0.00	0.00	0.00
Al	0.12	0.08	0.10	0.09	0.15	0.10	0.17	0.16	0.15	0.19	0.13	0.15
Cr	0.01	0.00	0.00	0.00	0.01	0.00	0.01	0.01	0.01	0.01	0.01	0.01
Fe^3	0.03	0.06	0.05	0.04	0.04	0.04	0.06	0.04	0.01	0.05	0.04	0.05
Fe^2	0.16	0.14	0.14	0.16	0.15	0.16	0.13	0.15	0.17	0.14	0.15	0.14
Mn	0.00	0.00	0.00	0.00	0.00	0.00	0.01	0.00	0.00	0.01	0.00	0.00
Mg	1.74	1.78	1.77	1.76	1.73	1.75	1.73	1.72	1.73	1.71	1.74	1.73
Ca	0.01	0.01	0.01	0.01	0.01	0.01	0.01	0.01	0.01	0.02	0.01	0.02
Na	0.00	0.00	0.00	0.00	0.00	0.00	0.00	0.00	0.00	0.00	0.00	0.00
Mg#	91.53	92.61	92.61	91.76	92.02	91.62	93.01	91.98	91.05	92.43	92.06	92.51
Cr#	5.35	4.80	4.53	4.87	6.25	0.00	5.56	5.88	6.25	5.00	7.14	6.25
Wo	0.54	0.38	0.39	0.56	0.53	0.52	0.53	0.53	0.52	1.07	0.53	1.06
En	91.04	92.26	92.24	91.24	91.53	91.15	92.51	91.49	90.58	91.44	91.58	91.53
Fs	8.42	7.36	7.36	8.19	7.94	8.33	6.95	7.98	8.90	7.49	7.89	7.41

Standards: SiO_2 (diopside), TiO_2 (rutile,Astimex, synthetic), Al_2O_3 (disthen, MAC),Cr_2O_3 (chromium Oxide, Astimex, synthetic), FeO (fayalite. USNM,Rockport), MnO (rhodonite, Astimex. Franklin, USA), MgO (Olivine,USNM, San Carlos), CaO (diopside), NiO (NiO, synthetic), Na_2O (jadeite), K_2O (K-Felspar). Opxt=Orthopyroxenite. Fe^{3+} and Fe^{2+} are calculate from stoichiometry. Mg# =100Mg/ (Mg+Fe^{2+}). Wo =Ca/ (Ca+Mg+Fe^{2+}). En= Mg/ (Ca+Mg+Fe^{2+}). Fs=Fe^{2+}/ (Ca+Mg+Fe^{2+}).

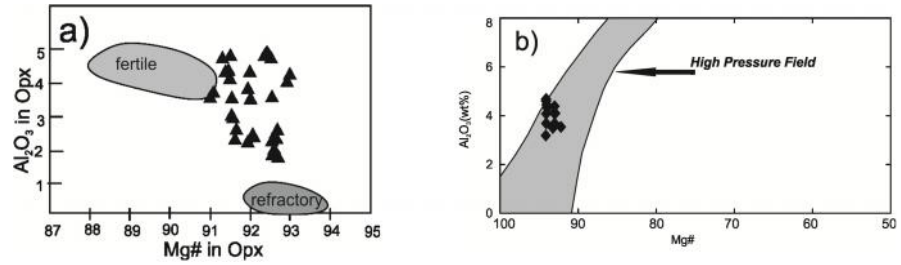

Figure 5. a) Mg# vs Al_2O_3 diagram for orthopyroxenes, Ab-Bid orthopyroxenes fall between fertile and refractory mantle. Data for fertile and refractory mantle are as Fig. 4. b) Mg# vs Al_2O_3 diagram for clinopyroxenes, Ab-Bid clinopyroxenes fall in high pressure field. High pressure field are from [20].

The nature of these lherzolites as residues of partial melting is shown by the amounts of CaO vs MgO diagram [Fig. 7a], Mg# vs Cr# diagram for spinels [Fig. 7b], and Cr# vs TiO_2 wt % in spinel, from Ab-Bid lherzolites [Fig. 7c]. So, all these diagrams show that the studied rocks passed 5-10 % partial melting. This evidence along with the higher values of incompatible elements (Na_2O, K_2O, TiO_2) compare with the well-known depleted mantle peridotites [23; 24] suggest that the studied lherzolites have been produced from low degrees of partial melting events.

On chondrite-normalized REE diagram [Fig. 8a], Ab-Bid lherzolites show spoon-shaped patterns with distinct flat trends for MREE and HREE, and clear depletion of LREE, suggest they have been passed low degrees of partial melting and then, they may have been affected by impregnation and enriched with La. In this figure, REE patterns of lherzolites, fall in upper part of the field of MORB peridotites and are very similar to refertalized refractory peridotites. Whole-

Table 5. Whole rock analyses of Ab–Bid lherzolites.

Sampel	A13	B29	R15	Z18	Z22
SiO_2	42.74	42.03	43.18	44.96	43.69
Al_2O_3	2.58	1.56	2.45	3.29	2.8
Fe_2O_3(T)	8.39	9.21	8.92	8.66	9.12
MnO	0.125	0.133	0.13	0.128	0.137
MgO	39.53	43.65	41.55	39.34	40.8
CaO	2.44	1.18	2.34	3.23	2.63
Na_2O	0.16	0.1	0.14	0.26	0.23
K_2O	0.02	0.03	0.02	0.02	0.03
TiO_2	0.06	0.03	0.06	0.095	0.074
P_2O_5	< 0.01	0.02	< 0.01	0.02	< 0.01
LOI	4.56	2.41	1.25	0.61	1.43
Total	100.6	100.3	100.1	100.6	101
Sc	12	8	12	15	12
V	58	34	60	76	60
Cr	2760	3060	2690	3010	2460
Co	98	112	104	103	110
Ni	2040	2360	2220	2070	2060
Cu	20	10	20	30	30
Zn	60	60	60	60	70
Ga	2	2	3	4	3
Ge	1	1	1.1	1	0.9
Sr	8	10	< 2	3	8
Y	2.2	1.5	2	3.1	1.9
Zr	3	5	2	4	4
Ag	0.6	0.7	0.6	0.5	< 0.5
Sb	0.4	0.4	0.4	0.3	0.5
Ba	4	24	3	< 3	15
La	0.14	3.44	0.14	0.16	0.36
Ce	0.18	6.28	0.13	0.24	0.48
Pr	0.03	0.77	0.03	0.06	0.06
Nd	0.28	2.72	0.28	0.43	0.35
Sm	0.15	0.42	0.16	0.21	0.15
Eu	0.065	0.115	0.047	0.099	0.067
Gd	0.23	0.32	0.21	0.36	0.23
Tb	0.04	0.05	0.04	0.07	0.05
Dy	0.28	0.25	0.3	0.5	0.33
Ho	0.07	0.05	0.07	0.11	0.07
Er	0.23	0.17	0.2	0.31	0.21
Tm	0.04	0.026	0.03	0.05	0.036
Yb	0.27	0.15	0.2	0.32	0.26
Lu	0.041	0.023	0.031	0.049	0.039
Ta	0.05	0.2	0.04	0.04	0.03
W	0.8	0.7	< 0.5	0.7	< 0.5
Tl	0.08	0.07	0.06	< 0.05	< 0.05
U	0.02	0.07	0.01	0.02	0.01

rock primitive mantle-normalized spider diagram [Fig. 8b] for Ab-Bid lherzolites resembles fertile abyssal peridotites, however the mobile right hand elements have enriched slightly probably due to the mantle metasomatism and refertilization.

Discussion

Lherzolites are essential members in ophiolite associations and mantle peridotite complexes and their mineralogical compositions suggest that they can form by various mechanisms. Some authors believe that they represent relatively fertile parts of the upper mantle which may have been affected by low degrees of partial melting events. Different mineralogical and

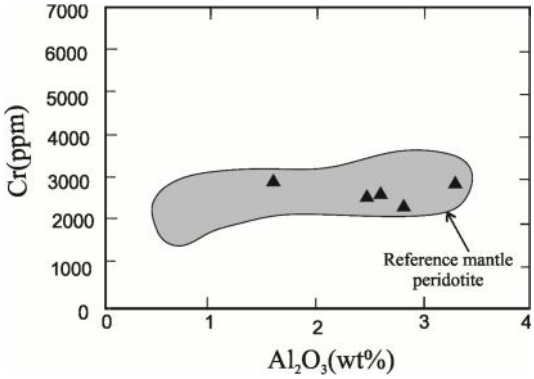

Figure 6. Al_2O_3 (Wt%) vs Cr (ppm) diagram for bulk rock compositions from Ab-Bid lherzolites. Reference mantle peridotite field are from [23].

chemical features support this idea in the lherzolites from oceanic or continental lithosphere related lherzolitic suits [5]. The other researchers [35] demonstrated that petrographical features and chemical variations are hardly consistent with a simple partial melting and may suggest that most of lherzolites observed at the Earth surface record refertilization processes. The refertilization mechanism also provides a key to understanding the paradoxical association of LREE-enriched harzburgites with LREE-depleted lherzolites often observed in mantle xenoliths and in tectonically-emplaced peridotites [4].

Extensive refertilization in the Western Alps and Betic peridotites is intrinsically related to the lithospheric thinning processes that led to mantle exhumation [18; 28; 22], which may suggest that large-scale refertilization can occurs in tectonically-emplaced orogenic peridotites. Similar LREE depletion in Ab-Bid lherzolites along with enrichment of La in these peridotites recognized in several spinel peridotite xenoliths [17]. These phenomena attributed to the magmatic refertilization of a previously depleted lithospheric mantle [17]. These evidences show spinel lherzolites can be secondary peridotites from more depleted harzburgites. Covariations of major-element values in whole rock and mineral compositions [Fig. 6 and Fig. 7a] in the Ab-Bid lherzolites are comparable to those observed in several suites of mantle rocks worldwide [5]. These covariations were generally ascribed to variable degrees of partial melt extraction [5; 6; 7], although in most cases variable degrees of refertilization of a refractory protolith would also account for the observed modal and chemical trends [4]. In the case of Ab-Bid, low degrees of partial melting event is supported by petrographical and chemical evidences.

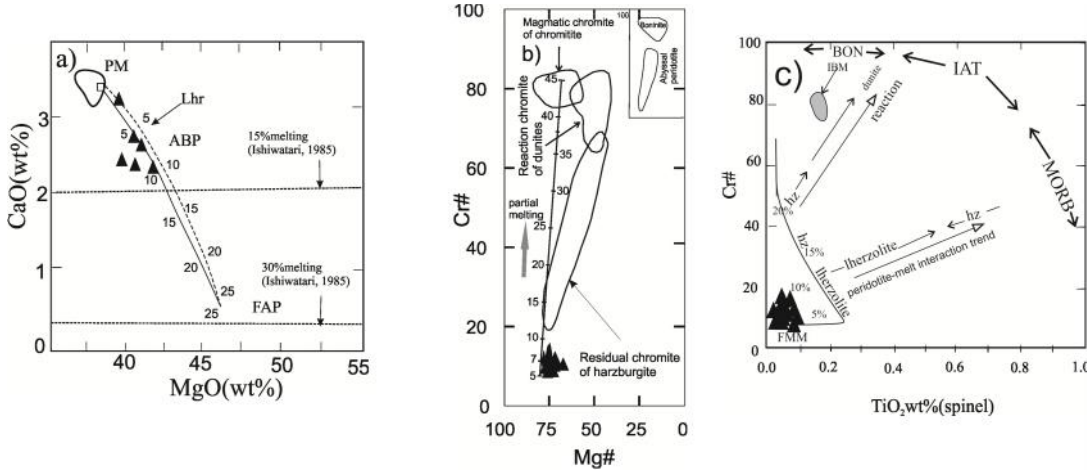

Figure 7. a) Bulk rock MgO vs CaO diagram for the Ab-Bid lherzolites [14]. b) Mg# vs Cr# diagram for spinels from Ab-Bid lherzolites. Fields are from [15]. c) Cr# vs TiO_2 wt % in spinel, from Ab-Bid lherzolites [26]. All diagrams show that the studied rock passed 5-10 % of partial melting.

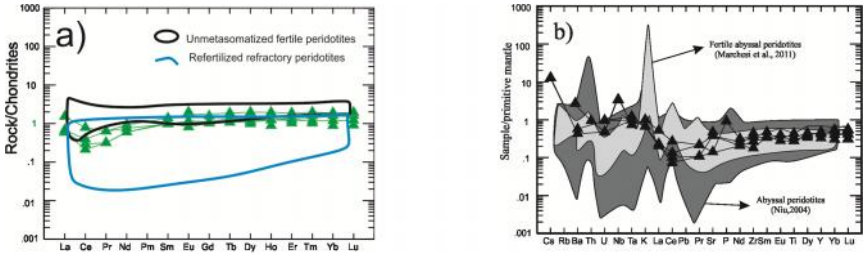

Figure 8. a) REE diagram for Ab-Bid lherzolites, nomalized to C1 chondrite. Data are from [5] and references therein for the unmetasomatized fertile peridotites from the Pyrenees, and from [5] for the refertilized refractory peridotites from the East Pacific Rise. b) Multi-element plot normalized to primitive mantle [36] for Ab-Bid lherzolites.

Small amounts of clinopyroxenes, presence of refractory olivine and orthopyroxene in these rocks [Fig. 7b,c] along with their REE pattern [Fig. 8], reveal that the Ab-Bid lherzolites have passed some degrees of partial melting process. Indeed, as shown in Fig. 7 , these peridotites can be formed by 5-10% partial melting.

There is a line of evidence in the Ab-Bid lherzolites suggest that these rocks have been partially melted and then affected by refertilization processes. In the field, the lherzolites cut by numerous pyroxenitic veins and dykes [Fig. 2b]. These intrusives can act as refertilization agents and change the mineralogy and chemical compositions of the host peridotites. In contrast with melt extraction, refertilization of a refractory protolith involving precipitation of Cr- and Al-bearing minerals, mostly spinel and pyroxenes. Under the microscope, there are textural features suggest that the Ab-Bid host lherzolites may have impregnated by a melt. These textures include (1) orthopyroxene porphyroclasts partly replaced by fine-grained secondary olivines [Fig. 3d], (2) embayments of orthopyroxene crystals by secondary olivine [Fig. 3d,e] and (3) interstitial extensions of spinel between adjacent crystals [Fig. 3f]. These mineralogical and textural characteristics have been identified as evidence of melt-rock interactions [30; 37]. Mineral chemical data from Ab-Bid lherzolites display some aspects of melt rock interaction for the host rocks. As shown in Fig. 4b, c and 5a chemical compositions of the studied orthopyroxenes and olivines fall in an area between refractory and fertile mantle. Influence of a melt on the peridotites can change the composition of their minerals and distributes them from refractory to fertile domains. Melt flow and melt–rock reaction in the mantle often leave chemical fingerprints in the host peridotites. The most outstanding feature which supports refertilization event on the Ab-Bid lherzolites is their REE patterns. Spoon-shaped REE patterns in these rocks [Fig. 6] are very similar to the well-known refertilized refractory peridotites.

LREE patterns observed at the lherzolite cannot be

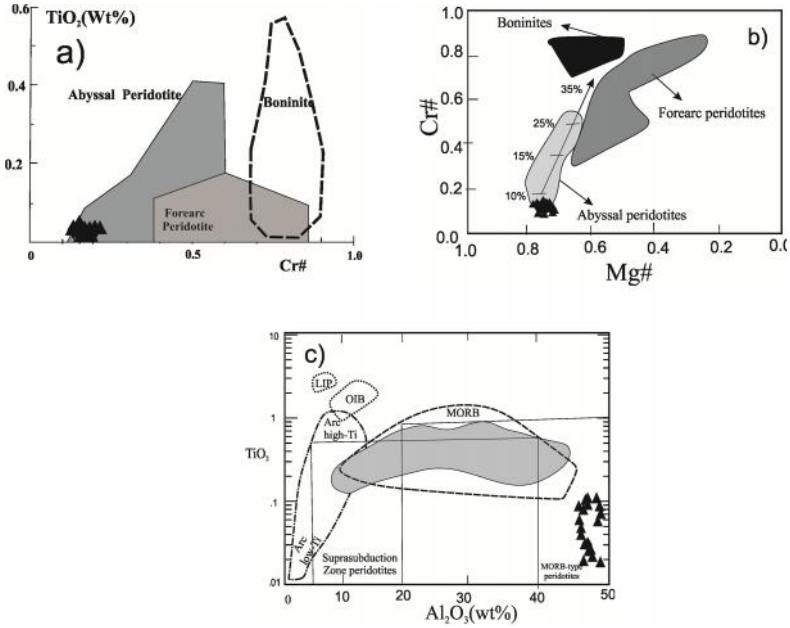

Figure 9. Compositional variations of spinels from Ab-Bid lherzolites in discrimination diagrams. a) Relationship between Cr# and TiO_2 content diagram which shows Ab-Bid lherzolites are similar to the Abyssal peridotites. General boninite field is from [34]. Abyssal peridotite and forearc peridotite [10]. b) Mg# vs Cr# discrimination diagram suggests that Ab-Bid lherzolites represent partially melted Abyssal peridotites. c) Diagrams of TiO_2 vs. Al_2O_3 (wt.%) of spinels from Ab-Bid lherzolites. Fields are from [16].

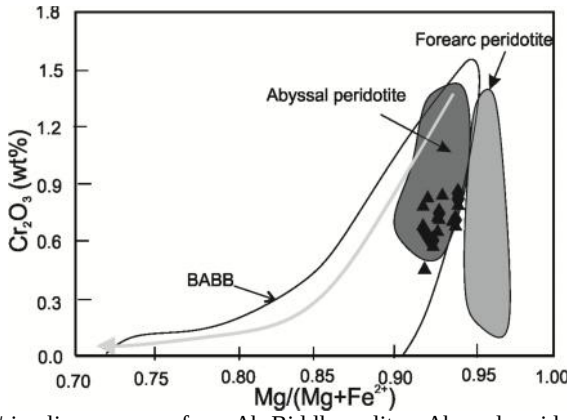

Figure 10. Cr_2O_3 (wt.%) vs. Mg# in clinopyroxene from Ab-Bid lherzolites. Abyssal peridotite field taken from [13], forearc peridotite field and Back-arc-basin basalt (BABB) field from [13].

explained by a simple partial melting model and provide further evidence for the refertilization process. Enrichment of highly incompatible elements (including LREE) at melt infiltration sites is indeed predicted by theoretical modelling of melt-consuming reactions combined with melt transport [6]. This enrichment results from segregation of volatile-rich small melt fractions moving ahead of melt-consuming reaction fronts. This mechanism, also referred to as "percolative fractional crystallization", was used to explain enriched LREE compositions in "cryptically" metasomatized mantle xenoliths [4]. In the Ab-Bid lherzolites, discordant pyroxenite veins and dykes [Fig. 2b] can act as a metasomatic agent.

whole rock and mineral compositions of the Ab-Bid lherzolites and discrimination diagrams show that these peridotites belong to the abyssal peridotites [Fig. 9a, b & Fig. 10], and in some diagrams they fall in the field of MORB type peridotites [Fig. 9c]. Ab-Bid complex consists one of the several ultramafic bodies in Esfandaghe-Hadji Abad ophiolite mélange. This mélange represents south-eastern continuation of the Kermanshah-Neyriz ophiolite belt [31]. Shafahi Moghadam [32, 33], represented ophiolites of this belt

as remnants of Neotethys oceanic lithosphere in central Iranian plate which have been detached during subduction of the Neotethys oceanic plate beneath central Iran at Mesozoic era, especially in the upper Cretaceous. Peighambari [27], considered that the Deh-sheikh ultramafic complex, which consists some parts of Esfandaghe-Hadji Abad ophiolite mélange is a part of oceanic lithosphere which is located above a subduction zone. Different evidences from the Ab-Bid lherzolites along with discrimination diagrams confirm these ideas. So, it is probably that the Ab-Bid peridotites have been made some parts of Neotethys oceanic lithosphere in this area and they have passed petrological processes relevant to this geological setting.

Conclusion

1- Ab-Bid ultramafic complex (South of Iran) contains harzburgite, dunite lherzolites and pyroxenitic veins.

2- Our results provide a unique set of features indicating that the Ab-Bid lherzolites were formed by polygenetic, multi-stage melting and refertilization events.

3- Refertilization reactions have changed the modal mineralogy and whole rock compositions of the studied lherzolites.

4- These peridotites and their host Ab-Bid ultramafic complex preserve evidence for the evolution of Neotethys oceanic lithosphere in South of Iran. Evidences show that this evolution involves partial melting of abyssal peridotites and then, refertilization processes in the sub-oceanic lithosphere occured.

Acknowledgements

We are grateful to professor Mr. Arvin (Shahid Bahonar University of Kerman) for making it possible to conduct quantitative electron microprobe analyses.

References

1. Alavi N.M. Tectonic of the Zagros, orognic belt of Iran, new data and interpretation. *Tectonophysics* **299**: 211-238(1984).
2. Azizian H., Naderi N., Navazi M., Posht Kohii M., Rashidi H. 1/100000 level Dolat – Abad Geological map *Geol. Sur. & Mineral. explor. Iran. Ser.* **346** (2007).
3. Bedard E., Hebert R., Guilmetta C., Lesage G., Wang C.S., Dostal J. Petrology and geochemistry of the sega and sangsang ophiolitic massifs, Yarlung Zangbo Suture Zone, Southern Tibet: Evidence for an arc-back-arc origin. *Lithos* **113**:48-67 (2009).
4. Beyer E.E., Griffin W.L., O'Reilly S.Y. Transformation of Archean lithospheric mantle by refertilization: evidence from exposed peridotites in the Western Gneiss Region, Norway. *J. petrol* **47**: 1611-1636(2006).
5. Bodinier J.L., Godard M. Orogenic, Ophiolitic and Abyssal Peridotites. *In: Carlson, R.W. (Ed.), Treatise. Geochem. Els. Sci. Ltd* **2**: 103-170 (2003).
6. Canil D. Mildly incompatible elemant in peridotite and the origins of mantle lithosphere. *Lithos* **77**: 375-393(2004).
7. Canil D., Johnston S.T., Mihalynuk M. Mantle redox in Cordilleran ophiolites as a record of oxygen fugacity during partial melting and the lifetime of mantle lithosphere. *Earth. Planet. Sci. let* **248**: 41-102(2006).
8. Carswell D.A. Picritic magma-residul dunite relationship in garnet peridotite at Kalskaret near Tafjord, south Norway. *Contrib. Mineral. Petrol* **19**: 97-124(1968).
9. Dawson J.B. A fertile harzburgite-garnet lherzolite transition: possible inferences for the roles of strain and metasomatism in upper mantle peridotites. *Lithos* **77**: 553-569(2004).
10. Dick H.J.B., Bullen T. Chromian spinel as a petrogenetic indicator in abyssal and alpine-type peridotites and spatially associated lavas. *Contrib. Mineral. Petrol* **86**: 54–76(1984).
11. Dilek Y. & Thy P. Island arc tholeiite to boninitic melt evolution of the Cretaceous Kızıldağ (Turkey) ophiolite model for multistage early arc–forearc magmatism in Tethyan subduction factories. *Lithos* **113**: 68–87(2009).
12. Hawkins J.W. and Allen J.F. Petrologic evolution of the Lau Basin, site 834-839, *in proc. ODP.Sci. Results* **135**:.J.W(1994).
13. Herzberg C. Geodynamic information in peridotite petrology. *J. Petrol* **45**: 2507–2530(2004).
14. Hirose K., Kawamoto T. Hydrous partial melting of lherzolite at 1GPa: the effect of H_2O on the genesis of basaltic magmas. *Earth. Planet. Sci. Lett* **133**: 463–473(1995).
15. Kamenetsky V.S., Crawford A.J., Meffre S. Factors controlling chemistry of magmatic spinel: an empirical study of associated olivine, Cr-spinel and melt inclusions from primitive rocks. *J. Petrol* **42**: 655–671(2001).
16. Kepezhinskas P.K., Defant M.J., Drummond M.S. Na metasomatism in the island-arc mantle by slab melt-peridotite interaction: evidence from mantle xenoliths in the North Kamchatka arc. *J. Petrol* **36**: 1505–1527(1995).
17. Lenoir X., Garrido C.J., Bodinier J.L., Dautria J.M., Gervilla F. The recrystallization front of the Ronda peridotite: evidence for melting and thermal erosion of subcontinental lithospheric mantle beneath the Alboran Basin. *J. Petrol* **42**: 141–158(2001).
18. McDonough W.F., Sun S.S. The composition of the Earth. *Chem. Geol* **12**: 223–253(1995).
19. Medaris L.G. High-pressure peridotites in south-western Oregon. *Bull.Geologic. Soc.Am* **83**: 41– 58(1972).
20. Mohajjel M., Fergusson C.I. and Shahandi M.R. Cretaceous Tertiary convergence and continental collision. Sanandaj-Sirjan zone, westeren Iran: *J. Asian. Earth. Sci* **21**: 397-412(2003).
21. Müntener O., Pettke T., Desmurs L., Meier M., Schaltegger U. Trace element and Nd-isotopic evidence

and implications for crust-mantle relationships. *Earth. Planet. Sci. Lett* **221**: 293–308(2004).
22. Orberger B., Lorand J.P., Girardeau J., Mercier J.C.C. and Pitragool S. Petrogenesis of ultramafic rocks and associated chromitites in the Nan Uttardit ophiolite, Northern Thailand. *Lithos* **35**: 153-182(1995).
23. Pagé P., Bédard J.H., Tremblay A. Geochemical variations in a depleted fore-arc mantle: The Ordovician Thetford Mines Ophiolite. *Lithos* **113**: 21–47(2009).
24. Parlak O., Rızaoğlu T., Bağcı U., Karaoğlan F. & Hock V. Tectonic significance of the geochemistry and petrology of ophiolites in southeast Anatolia Turkey. *Tectonophysic* **473**:173–187(2009).
25. Parkinson I.J., Pearce J.A. Peridotites from the Izu–Bonin–Mariana forearc (ODP leg 125): evidence for mantle melting and melt–mantle interaction in the supra-subduction zone setting. *J. Petrol* **39**: 1577–1618(1998).
26. Pearce J.A., Barker P.F., Edwards S.J., Parkinson I.J., Leat P.T. Geochemistry and tectonic significance of peridotites from the South Sandwich arc–basin system, South Atlantic. *Contrib. Mineral. Petrol* **139**: 36–53(2000).
27. Peighambari S., Ahmadipour H., Stosch H.G., Daliran F. Evidence for multi–stage mantle metasomatism at the Dehsheikh peridotite massif and chromite deposits of the Orzuieh coloured mélange belt, Southeasten Iran. *Ore. Geol. Rev* **39**: 245-264(2011).
28. Piccardo G.B., Muntener O., Zanetti A., Romarione A., Bruzzone S., Poggi E. & Spagnolo G. The Lenzo South Peridotite: melt/peridotite interaction in the mantle lithosphere of the Jurassic Ligurian Tethys. *Ofioliti* **29**: 37-62(2004).
29. Santos J.F., Scharer U., Ibarguchi J.I.G. and Girardeau J. Genesis of pyroxenite-rich peridotite at Cabo Ortegal (NW Spain):geochemical and Pb-Sr-Nd isotope data. *J. Petrol* **43**: 17-43(2002).
30. Seyler M., Lorand J.–P., Dick H.J.B., Drouin M. Pervasive melt percolation reactions in ultra-depleted refractory harzburgites at the Mid-Atlantic Ridge, 15_ 20°N: ODP Hole 1274. *Contrib. Mineral. Petrol* **153(3)**: 303–319(2007).
31. Shahabpour J. Tectonic evolution of the orogenic belt in the region located between Kerman and Neyriz. *J. Asian. Earth. Sci* **24**: 405–417 (2005). 32. Shafaii Moghadam H., Stern R.J., Rahgoshay M. The Dehshir ophiolite (Central Iran): Geochemical constraints on the origin and evolution of the Inner–Zagros ophiolite belt. *Bull. Geologic. Soc. AM* **122**: 1516-1547(2010).
33. Shafaii Moghadam H., Stern R.J., Chiaradia M. Geochemistry and tectonic evolution of the Late Cretaceous Gogher- Bft ophiolite, central Iran. *Lithos* **168-169**:33-47(2013).
34. Sobolev A.V. & Danyushevsky L.V. Petrology and geochemistry of boninites from the north termination of the Tonga trench: constraints on the generation conditions of primary high – Ca boninite magmas**.** *J. Petrol* **35**: 1183-1211(1994).
35. Stewart E., Lamb W., Newman J. and Tikoff. B. The petrological and geochemical evolution of early forearc mantle lithosphere: an example from the Red Hills ultramafic massif, New Zealand. *J. Petrol* **57**: 751-776(2016).
36. Sun S.S., McDonough W.F. Chemical and isotopic systematic of oceanic basalts: implications for mantle composition and processes. In: Saunders A.D., Norry M.J.(eds) Magmatism in the Ocean Basins. *Geol. Soc. Lon. Spec. Public* **42**: 313-345(1989).
37. Tamura A., Arai S., Andel E.S. Petrology and geochemistry of peridotites from TODP site U1309 at Atlantis massif. MAR 30N: micro- and macro- scale melt penetrations into peridotites. *Contrib. mineral. Petrol* **155(4)**: 491-509 (2008).
38. Uysal İ., Zaccarini F., Garuti G., Meisel T., Tarkian M., Bernhardt H.J. & Sadıklar M.B. Ophiolitic chromitites from the Kahramanmaraş area, southeastern Turkey: their platinum group elements (PGE) geochemistry, mineralogy and Os-isotope signature. *Ofioliti* **32**: 151–161 (2007).
39. Xiao W., Han C., Chao Y., Sun M., Zhao G., Shan Y. Transitions among Mariana, -Japan-, Cordillera-, and Alaska-type systems and their final luxtapositions leading to accretionary and collisional orogenesis. In kusky, T.M., Zhai, M.G., Xiao, W. (Eds). The evolving continents under – standing processes of continental Grawth. *Geol. Soc. Lond* **338**: 35-53(2010).
40. Zheng J.D., Griffin W.L., O Reilly S.Y., Yu C.M., Zhang H.F., Pearson N., Zhang M. Mechanism and timing of lithospheric modification and replacement beneath the eastern North Chaina Craton: Peridotitic xenoliths from the 100 Ma fuxin basalts and a regional synthesis. *Geochim. Cosmachim. Ac* **71**: 5203-5225(2007).